Flexible lipid bilayers in implicit solvent

Grace Brannigan
Department of Physics and Astronomy, University of California, Santa Barbara, California 93106-9530, USA

Peter F. Philips and Frank L. H. Brown
Department of Chemistry and Biochemistry, University of California, Santa Barbara, California 93106-9510, USA
(Received 21 December 2004; revised manuscript received 3 May 2005; published 26 July 2005)

A minimalist simulation model for lipid bilayers is presented. Each lipid is represented by a flexible chain of beads in implicit solvent. The hydrophobic effect is mimicked through an intermolecular pair potential localized at the "water"/hydrocarbon tail interface. This potential guarantees realistic interfacial tensions for lipids in a bilayer geometry. Lipids self-assemble into bilayer structures that display fluidity and elastic properties consistent with experimental model membrane systems. Varying molecular flexibility allows for tuning of elastic moduli and area per molecule over a range of values seen in experimental systems.

DOI: 10.1103/PhysRevE.72.011915 PACS number(s): 87.15.Aa, 87.14.Cc, 87.15.Ya, 87.16.Dg

Lipid bilayer biomembranes are of fundamental importance in cellular biology, and model membrane systems are fascinating physical systems in their own right. Simulation models for lipid bilayers have been developed over a range of resolutions (from fully atomistic descriptions to continuous elastic sheets) to address the many different length scales relevant to biological function and experimental study. The "mesoscopic" regime (~1–100 nm) is recognized as particularly relevant to the biophysical understanding of membrane systems [1].

Several coarse-grained bilayer models have been developed with the mesoscopic regime in mind [2–6]. Most of these depend upon explicit solvent to enforce bilayer stability. Coarse-grained solvent models do not provide detailed insight into the hydrophobic effect; the models are far too crude. Rather, such models provide a convenient means to enforce a bilayer stabilizing interfacial tension between solvent and lipid hydrocarbon tails (at considerable computational expense). Controlling the interfacial tension directly, without recourse to explicit solvent, would seem (if possible) a more direct route to the same end. A few solvent-free models [2,5,6] for bilayers do exist in the literature, but none include internal degrees of freedom for the lipids. Consequently, these models are unable to predict how molecular structure influences membrane properties, phase behavior, or realistic consequences of membrane heterogeneity. Such questions require flexible lipids to achieve even a qualitative level of understanding [1,7,8].

This paper presents a solvent-free lipid model that preserves the physics of lipid flexibility and hydrophobic attraction. The physical properties of the studied membranes closely resemble those of a solvated model with similar lipid resolution [3]. These results suggest that implicit solvent models may be appropriate for a wide class of problems in membrane biophysics. In particular, the computational simplicity of the present model makes it very attractive for future studies of heterogeneous bilayers, phase behavior, and related phenomena dependent on mesoscale lipid structure. The elementary approach adopted for mimicking hydrophobic attraction holds promise for extension to lipid models beyond those studied here.

Individual lipids are represented as semiflexible chains of five beads (Fig. 1). Bead 1 is identified as the hydrophilic head group, bead 2 is associated with the interface between hydrophilic and hydrophobic components, and beads 3–5 comprise the hydrophobic tail region. Bonded bead-bead distances are constrained to have length σ and bond angles are subject to a bending potential equivalent to that employed by Goetz and Lipowsky [3]:

$$U_{bend}(\theta) = c_{bend}\cos\,\theta, \tag{1}$$

where θ is one of three bond angles on the molecule (Fig. 1) and c_{bend} is a positive energetic constant. There is no energetic cost for dihedral rotations.

Individual beads interact through a combination of three different pair potentials:

$$U_{core}(r) = c_{core}(\sigma/r)^{12}, \tag{2}$$

$$U_{tail}(r) = -c_{tail}(\sigma/r)^{6}, \tag{3}$$

$$U_{int}(r) = -c_{int}(\sigma/r)^{2}, \tag{4}$$

where c_{core}, c_{tail}, and c_{int} are all positive energetic constants. With the exception of intramolecular bead pairs separated by less than three bonds, the repulsive core interaction acts between all bead pairs and the tail dispersion attraction acts between all tail-interface and tail-tail pairs. The soft interfacial attraction (discussed later) acts between all interface-interface pairs. The potentials are truncated at distances of $2\sigma, 2\sigma$, and 3σ for the core, tail, and interfacial interactions, respectively, and shifted to ensure continuity of the potential. Truncation of the otherwise long ranged U_{int} is an essential component of the interaction and should not be viewed as an approximation to a true r^{-2} potential.

Though U_{core} and U_{tail} are standard, U_{int} has an unusual form and we include no explicit treatment of electrostatics. Our model is clearly empirical, but as detailed below provides an uncanny correspondence with true lipid bilayer systems.

The results described below were obtained using the values $k_BT=0.9\epsilon, c_{core}=0.4\epsilon, c_{tail}=1.0\epsilon$, and $c_{int}=3.0\epsilon$ with

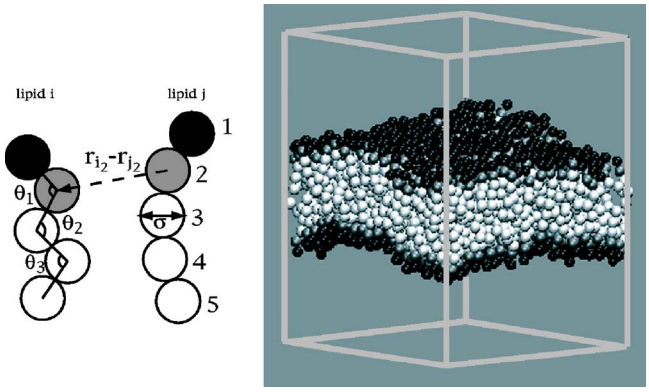

FIG. 1. (Color online) Left: Definition of parameters used in model. Right: Sample conformation of tensionless membrane with 800 lipid molecules ($c_{bend}=7\epsilon$). Hydrophilic head beads are black, interface beads are gray, and hydrophobic tail beads are white. Simulations presented in this work employ five bead lipids exclusively. Modification to longer lipids with more tail beads is possible and straightforward.

c_{bend} varied between 5.0ϵ and 10.0ϵ. Low values of $c_{bend}(<5\epsilon)$ resulted in bilayers with a tendency to form pores and high values of $c_{bend}(>15\epsilon)$ gave rise to bilayers with ordered structure. The reduced units are calibrated by mandating that the simulations are conducted at 300 K and that the largest observed area per molecule (at $c_{bend}=5.0\epsilon$) corresponds to about 0.7 nm^2. This results in the unit scale $\epsilon=2.75$ kJ/mol and $\sigma=0.75$ nm.

Simulations were carried out by the Metropolis Monte Carlo method using standard moves for short chains [9] and an additional move that attempted translation of an entire molecule. Stability was verified by bilayer assembly at constant box dimensions from a random configuration of 128 molecules (Fig. 2). All other simulations were conducted in the constant-vanishing-tension–constant-volume ensemble [6,10]. Crystalline bilayers of 800 molecules were allowed to equilibrate prior to data collection, and fluidity was verified by lateral diffusion. A density of 0.07 lipids per σ^3 was used throughout, which prevents the membrane from interacting with its periodic images in the z direction. During the course of simulation, lipids occasionally leave the bilayer to explore the box and later reenter the bilayer—i.e., at equilibrium

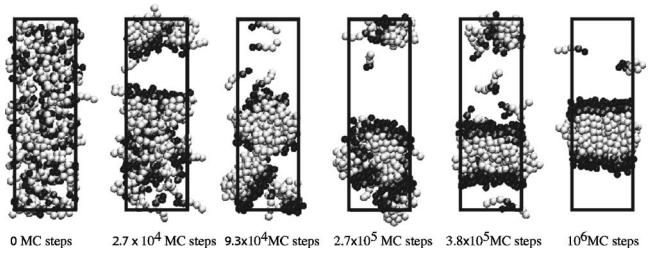

FIG. 2. Self-assembly of a bilayer patch of 128 lipids ($c_{bend}=7\epsilon$) in a box with constant dimensions $L_x=L_y=8.6\sigma, L_z=25\sigma$, and periodic boundary conditions. The chosen area corresponds to that assumed by a preassembled bilayer at zero tension. Each Monte Carlo (MC) step includes (on average) an attempt to translate each bead in the simulation.

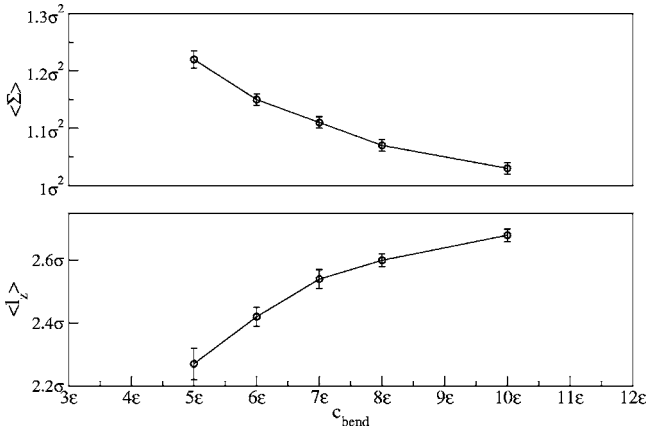

FIG. 3. Projected area per molecule (top) and leaflet thickness-(bottom) as a function of molecular bending coefficient c_{bend} for membranes under zero tension. The volume $\langle \Sigma l_z \rangle$ is insensitive to c_{bend}. Lines are to guide the eye.

monomers and bilayer lipids exchange [(0-3) % monomers depending on c_{bend}].

In membranes with $c_{bend}=(5–10)\epsilon$, molecular area scales inversely with molecular rigidity, but a simultaneous increase in bilayer thickness preserves membrane volume (Fig. 3). The thickness of a leaflet is defined by the average z distance between a molecule's interface bead and its final tail bead: $\langle l_z \rangle = \langle (\vec{r}_5 - \vec{r}_2) \cdot \hat{z} \rangle$. Unsurprisingly, stiffer chains offer greater resistance to compression in length, resulting in thicker membranes (Fig. 3). In model membrane systems, zero-tension areas per molecule range from about 0.596 nm^2 for dimyristoylphosphatidylcholine(DMPC) to 0.725 nm^2 for dioleoylphosphatidylcholine(DOPC) [11]. Using our model, we achieve a 20% range (0.57–0.68 nm^2) in areas by adjusting the chain stiffness alone.

A linearly elastic sheet can be described by [12]

$$\tilde{\gamma} = k_A (L^2 - A_0)/A_0 \tag{5}$$

where $\tilde{\gamma}$ is the surface tension, k_A is the compressibility modulus, L^2 is the projected area, and A_0 is the zero-tension area. Although the simulation algorithm maintains a constant thermodynamic tension γ, $\tilde{\gamma}$ represents the mechanical surface tension, which is measurable via the virial stress tensor [13] and fluctuates throughout the simulation (with sufficient averaging, $\langle \tilde{\gamma} \rangle = \gamma$). We measure k_A by linear regression of $\tilde{\gamma}$ vs L^2 [3]; we found that this method yields equivalent results to a measurement via the thermal fluctuations, as in Ref. [14], but converges more quickly. k_A values range from $(5\pm4)\epsilon/\sigma^2$ for $c_{bend}=5\epsilon$ to $(28\pm9)\epsilon/\sigma^2$ for $c_{bend}=10\epsilon$. Given our unit calibration, these values correspond to 40–224 mJ/m^2, in good agreement with single-component phospholipid bilayers, which typically range from 60 to 270 mJ/m^2 [8,15]. In contrast to the results of Refs. [16,18], we found that k_A measurements for systems with 800 and 128 molecules agreed within error bars, although the smaller system measurements converged far more quickly.

While k_A provides a direct link to experiment, more detailed microscopic information is obtained by measuring the stress profile across the bilayer [3,19]. Defining the local

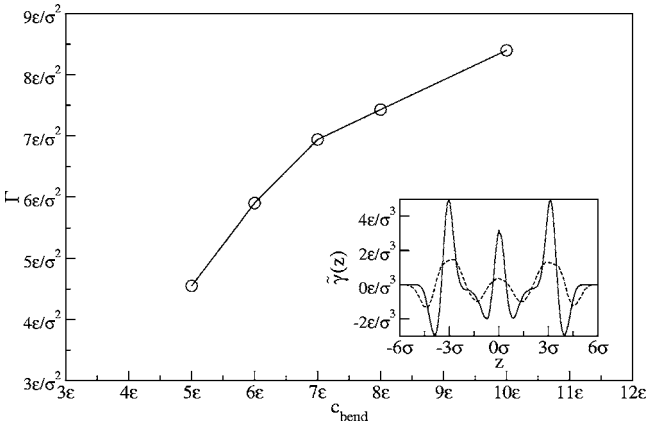

FIG. 4. Interfacial tension as defined in Eq. (6). Error bars are smaller than symbol size and line is to guide the eye. Inset: Stress profile for systems with 128 (solid) and 800 molecules (dashed) showing the same pattern of peaks and valleys as observed in a similar solvated model [3]. Profiles correspond to systems with $c_{bend}=7\epsilon$.

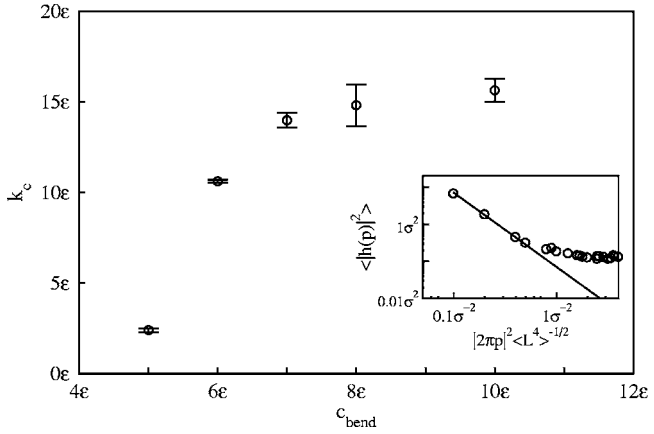

FIG. 5. Membrane bending rigidity (k_c) as a function of molecular rigidity (c_{bend}). Data points represent a fit to the four longest wavelength modes; error bars represent the standard error in the fit. Each data point corresponds to about one week of computation on a 2.3 GHz Athlon CPU. Inset: Spectrum, for $c_{bend}=7\epsilon$, where the line is a fit to Eq. (7) with $k_c=13.9\epsilon$.

mechanical tension as a function of displacement z relative to the bilayer center of mass $\tilde{\gamma}(z)=P_n(z)-P_t(z)$ (the difference between normal and tangential pressures), we measure the stress profile for systems with $N=128$ and 800 molecules (Fig. 4 inset). The profiles agree qualitatively with those obtained from fully atomic models [19] and nearly quantitatively with those obtained from solvated membranes also composed of five bead chains [3]. The peaks of high positive tension correspond to the positions of the interface beads, indicating that these beads are holding the bilayer together, against the lateral repulsions of hydrophilic heads and third and fourth beads. Undulations significantly smooth out the profile, even in moderately sized bilayers with 800 molecules.

In our model, a strong attraction between interface beads mimics the hydrophobic effect. Since all "solvent" effects of our model are incorporated within U_{int}, we define the effective interfacial tension by the interfacial contribution to the virial tension:

$$\Gamma=\frac{1}{2}\sum_{i<j}\left\langle\frac{r_{ij}^2-3z_{ij}^2}{2L^2r_{ij}}\frac{\partial U_{int}(r_{ij})}{\partial r_{ij}}\right\rangle, \tag{6}$$

where the sum is over all distinct pairs of interface beads. The factor of $1/2$ corresponds to the two interfaces present in a bilayer and Γ is thus defined in the usual sense of the interfacial tension [21]. The surface pressure for each leaflet is given by the difference between total and interfacial tensions $\Pi=\Gamma-\langle\tilde{\gamma}\rangle/2$ so that $\Pi=\Gamma$ in the zero-stress state simulated here. We measure values of $\Gamma=(4\text{–}8)\epsilon/\sigma^2(32\text{–}65\ \mathrm{mJ/m^2})$ (Fig. 4). Theoretical estimates range from 20 to 50 $\mathrm{mJ/m^2}$ [7,20,21]).

The functional form chosen for U_{int} in our model is empirical, and was identified through trial and error motivated by our previous experience with rigid lipid models [6]. The approximate magnitude of c_{int} given this functional form is dictated by physical necessity: $c_{int}=3.0\epsilon$ leads to a stable fluid phase for a variety of c_{bend} values and physically reasonable interfacial tensions. Connection between U_{int} and the hydrophobic effect is established solely on this basis.

Membranes display obvious long wavelength fluctuations (Fig. 1) that we have quantified via the fluctuation spectrum [2,3]. In the constant-zero-tension ensemble, a flexible fluid sheet is expected to display undulations consistent with [6]

$$\langle|h(\vec{p})|^2\rangle=\frac{k_BT}{k_c}\frac{\langle L^4\rangle}{(2\pi|\vec{p}|)^4}, \tag{7}$$

where k_c is the bending rigidity, $h(x,y)$ is the local height of the membrane midplane, $h(\vec{p})=(1/L)\int dx\,dy\,h(x,y)e^{i2\pi\vec{p}\cdot\vec{r}/L}$ and the components of $\vec{p}$ are $(\pm1,\pm2,\ldots,\pm n/2)$. The inferred rigidities are shown in Fig. 5 with a representative spectrum shown in the inset. Wavelengths shorter than the membrane thickness clearly do not follow Eq. (7) and have been excluded from the fit as discussed extensively in prior work [3,16,17]. Bending rigidities are in the range $k_c=(2.5\text{–}16)\epsilon$ [approx. $(1\text{–}8)\times10^{-20}J$]. The more flexible systems are consistent with experimental measurements of digalactosyldiacylglycerol(DGDG), while the stiffer systems agree well with measurements of dilauroylphosphatidylcholine(DLPC) and DMPC [22]. Stiffer molecules lead to stiffer membranes; this can be partially attributed to the increase in both compressibility modulus and membrane thickness. It has been suggested that one should generally expect $k_c=k_Ad^2/b$, where d is the bilayer thickness and b is a dimensionless constant [1,3,8]. We measure $b\sim60$ for the model presented here, well within the limits seen in other simulation models ($b\sim4$ to $b\sim100$) [3,6,16–18] and experiment [8].

Mesoscopic models provide a link between atomic level detail and macroscopic physical properties. The present description incorporates a level of realism previously lacking in implicit solvent models for lipid bilayers and should allow

for detailed studies of biophysical questions where solvated models are computationally prohibitive. Additionally, the physical picture afforded by this model is very much in the spirit of analytical theories that seldom consider water explicitly. Modeling at this level of detail should provide a critical link between experiment, theory, and atomistic simulations. The simulation of inhomogeneous membrane surfaces (with multiple lipid species and protein inclusions) is especially promising and is currently under investigation.

This work was supported in part by the Petroleum Research Fund of the American Chemical Society (Grant No. 42447-G7) and the National Science Foundation (Grant No. MCB-0203221 and No. CHE-0321368).

[1] M. Bloom, E. Evans, and O. G. Mouritsen, Q. Rev. Biophys. **24**, 293 (1991).
[2] J.-M. Drouffe, A. C. Maggs, and S. Leibler, Science **254**, 1353 (1991).
[3] R. Goetz and R. Lipowsky, J. Chem. Phys. **108**, 7397 (1998); R. Goetz, G. Gompper, and R. Lipowsky, Phys. Rev. Lett. **82**, 221 (1999).
[4] B. Smit, P. A. J. Hilbers, K. Esselink, L. A. M. Rupert, N. M. van Os, and A. G. Schlijper, J. Phys. Chem. **95**, 6361 (1991); R. D. Groot and K. L. Rabone, Biophys. J. **81**, 725 (2001). G. Ayton, S. G. Bardenhagen, P. McMurty, D. Sulsky, and G. A. Voth, J. Chem. Phys. **114**, 6913 (2001); J. C. Shelley, M. Y. Shelley, R. C. Reeder, S. Bandyopadhyay, and M. L. Klein, J. Phys. Chem. B **105**, 4464 (2001); T. Soddemann, B. Dunweg, and K. Kremer, Eur. Phys. J. E **6**, 409 (2001); J. Shillcock and R. Lipowsky, J. Chem. Phys. **117**, 5048 (2002); S. Yamamoto, Y. Maruyama, and S.-A. Hyodo, *ibid.* **116**, 5842 (2002); L. Rekvig, M. Kranenburg, J. Vreede, B. Hafskjold, and B. Smit, Langmuir **19**, 4897 (2003).
[5] H. Noguchi and M. Takasu, J. Chem. Phys. **115**, 9547 (2001); O. Farago, *ibid.* **119**, 596 (2003).
[6] G. Brannigan and F. L. H. Brown, J. Chem. Phys. **120**, 1059 (2004); G. Brannigan, A. C. Tamboli, and F. L. H. Brown, *ibid.* **121**, 3259 (2004).
[7] J. F. Nagle, Annu. Rev. Phys. Chem. **31**, 157 (1980); , Faraday Discuss. Chem. Soc. **81**, 151 (1986); A. Ben-Shaul, in *Structure and Dynamics of Membranes*, edited by R. Lipowsky and E. Sackmann (Elsevier Science, Amsterdam, 1995), Vol. 1.
[8] W. Rawicz, K. Oldbrich, T. McIntosh, D. Needham, and E. Evans, Biophys. J. **79**, 328 (2000).
[9] X. J. Li and Y. C. Chiew, J. Chem. Phys. **101**, 2522 (1994); A. Baumgartner and K. Binder, *ibid.* **71**, 2541 (1979).
[10] M. Venturoli and B. Smit, PhysChemComm **10**, 7397 (1999).
[11] J. F. Nagle and S. Tristram-Nagle, Biochim. Biophys. Acta **1469**, 159 (2000).
[12] E. A. Evans and R. Skalak, *Mechanics and Thermodynamics of Biomembranes* (CRC Press, Boca Raton, FL, 1980).
[13] D. Frenkel and B. Smit, *Understanding Molecular Simulation: From Algorithms to Applications*, 2nd ed. (Academic Press, New York, 2002).
[14] S. E. Feller and R. W. Pastor, J. Chem. Phys. **111**, 1281 (1999).
[15] E. Sackmann, in *Structure and Dynamics of Membranes* (Ref. [7]).
[16] S. J. Marrink and A. E. Mark, J. Phys. Chem. **105**, 6122 (2001).
[17] E. Lindahl and O. Edholm, Biophys. J. **79**, 426 (2000).
[18] W. den Otter and W. Briels, J. Chem. Phys. **118**, 4712 (2003).
[19] E. Lindahl and O. Edholm, J. Chem. Phys. **113**, 3882 (2000).
[20] D. Marsh, Biochim. Biophys. Acta **1286**, 183 (1996).
[21] J. Israelachvili, *Intermolecular and Surface Forces* (Wiley, New York, 1992).
[22] U. Seifert and R. Lipowsky, in *Structure and Dynamics of Membranes* (Ref. [7]).